# Solvent-Induced *syn*−*anti* Rotamerization of 2-(2′-Pyridyl)indole and the Structure of its Alcohol Complexes

**A. Kyrychenko,[†,§] J. Herbich,[†] F. Wu,[‡] R. P. Thummel,[‡] and J. Waluk*[,†]**

*Contribution from the Institute of Physical Chemistry, Polish Academy of Sciences, Kasprzaka 44, 01-224 Warsaw, Poland, and Department of Chemistry, University of Houston, Houston, Texas 77204-5641*

*Received June 1, 1999. Revised Manuscript Received November 9, 1999*

**Abstract:** Conformational changes caused by specific interactions with protic solvents were studied for 2-(2′-pyridyl)indole and related compounds. Both *syn* and *anti* rotameric forms are possible for 2-(2′-pyridyl)-indole. Only the *syn* conformers are able to form cyclic, doubly hydrogen-bonded complexes with protic solvents. These cyclic solvates undergo efficient fluorescence quenching due to photoinduced double proton transfer and internal conversion. This feature makes it possible to distinguish between the two rotamers and to determine their relative abundance. In aprotic solvents, only the *syn* form is detected. On the contrary, fluorescence measurements reveal that in alcohols about 80% of the excited-state population are due to the *anti* conformer. Similar results are obtained for the ground state from NMR NOE experiments, which imply that no interconversion between the two forms occurs in the excited state. Ab initio calculations predict that the *syn* form should be more stable by about 4.3 kcal/mol. Therefore, the data obtained in alcohol solvents show that the reversal of the *syn*/*anti* relative stability is due to hydrogen bonding to the solvent. These conclusions are confirmed by experiments performed for the N-methylated derivative, for bridged 2-(2′-pyridyl)indoles which can only exist in the *syn* form, and for 2-(4,6-dimethyl-2′-pyrimidyl)indole, where *syn* and *anti* conformers are identical. In bulk water solutions no evidence for *syn* → *anti* rotamerization was found. However, the process was detected in acetonitrile/water mixtures.

## Introduction

Bifunctional molecules possessing both proton donor and acceptor groups may reveal simultaneous enhancement of acidity and basicity upon electronic excitation. This enhancement can lead to proton transfer from the donor to the acceptor site. If the location of the donor and acceptor sites precludes a direct proton transfer, the shift can still occur as a biprotonic process through a hydrogen-bonded bridge formed between the two sites. A prototype for such systems is 7-azaindole (**7AI**), which can form cyclic hydrogen-bonded dimers, or complexes with hydroxylic partners. Both types of structures exhibit excited-state double proton transfer,[1] and considerable study has been devoted to the structural and kinetics aspects of this process.[2−31] Nevertheless, fundamental questions remain regarding the structure of the reactive species and the rate-limiting step in alcohols and water. To better understand the mechanism of

* Correspondence author. Telephone (+4822) 632 7269. Fax: (+48) 391 20 238. E-mail: waluk@ichf.edu.pl.

† Polish Academy of Science.

‡ University of Houston.

§ Permanent address: Research Institute for Chemistry, Kharkov State University, 4, Svobody Sq., 310077 Kharkov, Ukraine.

(1) Taylor, C. A.; El-Bayoumi, M. A.; Kasha, M. *Proc. Natl. Acad Sci. U.S.A.* **1969**, *63*, 253.

(2) Ingham, K. D.; El-Bayoumi, M. A. *J. Am. Chem. Soc.* **1974**, *96*, 1674.

(3) Ingham, K. C.; Abu-Elgheit, M.; El-Bayoumi, M. A. *J. Am. Chem. Soc.* **1971**, *93*, 5023.

(4) Hetherington, W. M., III; Micheels, R. M.; Eisenthal, K. B. *Chem. Phys. Lett.* **1979**, *66*, 230.

(5) Share, P. E.; Sarisky, M. J.; Pereira, M. A.; Repinec, S. T.; Hochstrasser, R. M. *J. Lumin.* **1991**, *48/49*, 204.

(6) Bulska, H.; Chodkowska, A. *J. Am. Chem. Soc.* **1980**, *102*, 3259.

(7) Bulska, H.; Grabowska, A.; Pakuła, B.; Sepioł, J.; Waluk, J.; Wild, U. P. *J. Lumin.* **1984**, *29*, 65.

(8) Fuke, K.; Kaya, K. *J. Phys. Chem.* **1989**, *93*, 614.

(9) Douhal, A.; Kim, S. K.; Zewail, A. H. *Nature* **1995**, *378*, 260.

(10) Douhal, A.; Guallar, V.; Moreno, M.; Lluch, J. M. *Chem. Phys. Lett.* **1996**, *256*, 370.

(11) Chachissvilis, M.; Fiebig, T.; Douhal, A.; Zewail, A. H. *J. Phys. Chem. A* **1998**, *102*, 669.

(12) Folmer, D. E.; Poth, L.; Wisniewski, E. S.; Castleman, A. W., Jr. *Chem. Phys. Lett.* **1998**, *287*, 1.

(13) Takeuchi, S.; Tahara, T. *J. Phys. Chem. A* **1998**, *102*, 7740.

(14) Takeuchi, S.; Tahara, T. *Chem. Phys. Lett.* **1997**, *277*, 340.

(15) Lopez-Martens, R.; Long, P.; Solgadi, D.; Soep, B.; Syage, J.; Millie, Ph. *Chem. Phys. Lett.* **1997**, *273*, 219.

(16) Nakajima, A.; Hirano, M.; Hasumi, R.; Kaya, K.; Watanabe, H.; Carter, C. C.; Williamson, J. M.; Miller, T. A. *J. Phys. Chem. A* **1997**, *101*, 392.

(17) Avouris, P.; Yang, L. L.; El-Bayoumi, M. A. *Photochem. Photobiol.* **1976**, *24*, 211.

(18) Smirnov, A. V.; English, D. S.; Rich, R. L.; Lane, J.; Teyton, L.; Schwabacher, A. W.; Luo, S.; Thornburg, R. W.; Petrich, J. W. *J. Phys. Chem. B* **1997**, *101*, 2758.

(19) McMorrow, D.; Aartsma, T. J. *Chem. Phys. Lett.* **1986**, *125*, 581.

(20) Moog, R. S.; Bovino, S. C.; Simon, J. D. *J. Phys. Chem.* **1988**, *92*, 6545.

(21) Konijnenberg, J.; Huizer, A. H.; Varma, C. A. G. O. *J. Chem. Soc., Faraday Trans. 2* **1988**, *84*, 1163.

(22) Moog, R. S.; Maroncelli, M. *J. Phys. Chem.* **1991**, *95*, 10359.

(23) Herbich, J.; Sepioł, J.; Waluk, J. *J. Mol. Struct.* **1984**, *114*, 329.

(24) Chapman, C. F.; Maroncelli, M. *J. Phys. Chem.* **1992**, *96*, 8430.

(25) Mente, S.; Maroncelli, M. *J. Phys. Chem. A* **1998**, *102*, 3860.

(26) Chen, Y.; Gai, F.; Petrich, J. W. *J. Am. Chem. Soc.* **1993**, *115*, 10158.

(27) Chen, Y.; Gai, F.; Petrich, J. W. *Chem. Phys. Lett*, **1994**, *222*, 329.

(28) Chou, P.-T.; Martinez, M. L.; Cooper, W. C.; Collins, S. T.; McMorrow, D. P.; Kasha, M. *J. Phys. Chem.* **1992**, *96*, 5203.

(29) Chen, Y.; Rich, R. L.; Gai, F.; Petrich, J. W. *J. Phys. Chem.* **1993**, *97*, 1770.

(30) Chang, C.-P.; Wen-Chi, H.; Meng-Shin, K.; Chou, P.-T.; Clements, J. H. *J. Phys. Chem.* **1994**, *98*, 8801.

(31) Chou, P.-T.; Wei, C.-Y.; Chang, C.-P.; Meng-Shin, K. *J. Phys. Chem.* **1995**, *99*, 11994.

10.1021/ja991818r CCC: $19.00 
Published on Web 03/14/2000

**Chart 1**

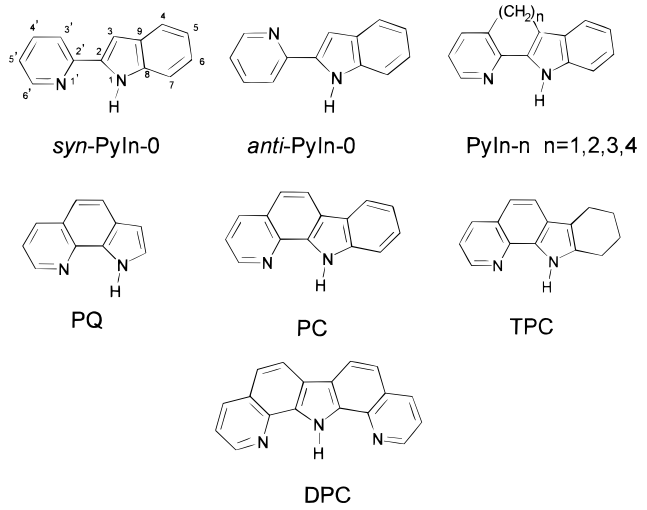


proton transfer in alcohol solvates, we have recently studied a large family of bifunctional molecules resembling **7AI** due to the presence of an H-bond donor NH group and an H-bond acceptor pyridine nitrogen (Chart 1). The compounds investigated included 2-(2′-pyridyl)indoles (**PyIn-0**−**PyIn-4**),[32−35] dipyrido[2,3-*a*:3′,2′-*i*]carbazole (**DPC**),[36] 1-H-pyrrolo[3,2-*h*]-quinoline (**PQ**), 7,8,9,10-pyrido[2,3-*a*]carbazole (**TPC**), and pyrido[2,3-*a*]carbazole (**PC**).[37] An independent study of **PQ** has been recently reported.[38] It was found that the photophysical behavior of all these molecules changes dramatically in alcohol solutions: very strong fluorescence quenching is observed, accompanied by the appearance of a new, low-energy emission, which is assigned to a tautomer resulting from excited state double proton transfer. Both tautomerization and $S_1 \rightarrow S_0$ internal conversion were found to be important channels for rapid excited-state deactivation in alcohols.

In a series of 2-(2′-pyridyl)indoles, intriguing quantitative differences were observed between the parent, unbridged compound, **PyIn-0**, and its bridged derivatives, **PyIn-1**, **PyIn-2**, **PyIn-3**, and **PyIn-4**. The fluorescence of the bridged compounds was nearly 2 orders of magnitude weaker in alcohols than in nonpolar and polar aprotic solvents. For **PyIn-0**, the quenching in alcohols was also observed, but the corresponding intensity decrease was much smaller, less than 4-fold.[32] Comparison of the positions of the fluorescence maxima in alcohols and other hydrogen-bonding solvents, such as pyridine, showed a difference for **PyIn-0**, while in the bridged derivatives, the spectra were very similar for both kinds of solvents.[33] Different patterns were also noticed in the absorption curves obtained while titrating solutions in nonpolar solvents with alcohols. Clear isosbestic points were observed for bridged compounds, but not for **PyIn-0**.[32]

**Chart 2**

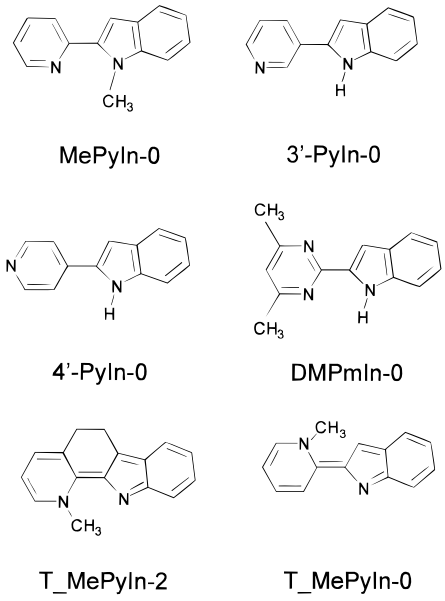


The purpose of the present work is to show that all of these findings can be explained by the presence, in alcohol solutions, of two rotamers of **PyIn-0**. In aprotic solvents, only the *syn* conformer is observed. The *anti* rotamer, absent in both polar and nonpolar aprotic media, becomes dominant in alcohols. The effect is due to specific, hydrogen-bonding interactions with alcohol molecules, since for the isolated **PyIn-0** the *syn* rotamer is thermodynamically more favorable. The results also demonstrate that in bulk alcohols, the formation of two separate hydrogen bonds in the *anti* conformer, involving two alcohol molecules, is preferred over a cyclic structure involving a single alcohol molecule. On the contrary, at low alcohol concentrations in nonpolar solvents, 1:1 complexes formed by the *syn* conformer are prevalent.

The behavior in bulk water was found to be different than in bulk alcohols. No evidence for *anti* rotamers was found. However, rotamerization was detected in mixed water/acetonitrile solutions.

These conclusions are supported by studies of several model molecules (Chart 2): (i) **MePyIn-0** (an N-methylated derivative of **PyIn-0**); (ii) two isomers of **PyIn-0**: 2-(3′-pyridyl)indole (**3′-PyIn-0**) and 2-(4′-pyridyl)indole (**4′-PyIn-0**), of which only the former can exist as *syn* and *anti* rotamers; (iii) 2-(4,6-dimethyl-2′-pyrimidyl)indole (**DMPmIn-0**), for which *syn* and *anti* conformers are identical; 1-methyl-3,3′-dimethylene-2-(2′-indolenylidene)-1,2-dihydropyridine (**T_MePyIn-2**) and 1-methyl-2-(2′-indolenylidene)-1,2-dihydropyridine (**T_MePyIn-0**), models for tautomeric species of **PyIn-2** and **PyIn-0**, respectively.

## Experimental and Computational Details

The synthesis and purification of 2-(2′-pyridyl)indoles and the chemical models of their tautomers have been described elsewhere.[34,39,40] The preparation of 2-(3′-pyridyl)indole and 2-(4′-pyridyl)indole has been reported in the literature.[41]

**2-[2′-(4′,6′-Dimethylpyrimidyl)]-indole** (**DMPmIn-0**)**.** A mixture of the phenylhydrazone of 2-acetyl-4,6-dimethylpyrimidine[42] (0.30 g,

(32) Herbich, J.; Rettig, W.; Thummel, R. P.; Waluk, J. *Chem. Phys. Lett.* **1992**, *195*, 556.
(33) Herbich, J.; Waluk, J.; Thummel, R. P.; Hung C. Y. *J. Photochem. Photobiol., A* **1994**, *80*, 157.
(34) Herbich, J.; Hung, C.-Y.; Thummel, R. P.; Waluk, J. *J. Am. Chem. Soc.* **1996**, *118*, 3508.
(35) Dobkowski, J.; Herbich, J.; Galievsky, V.; Thummel, R. P.; Waluk, J. *Ber. Bunsen-Ges. Phys. Chem.* **1998**, *3*, 469.
(36) Herbich, J.; Dobkowski, J.; Thummel, R. P.; Hegde, V.; Waluk, J. *J. Phys. Chem. A* **1997**, *101*, 5839.
(37) (a) Kyrychenko, A.; Herbich, J.; Izydorzak, M.; Wu, F.; Thummel, R. P.; Waluk, J. *J. Am. Chem. Soc.* **1999**, *121*, 1179. (b) Kyrychenko, A.; Herbich, J.; Izydorzak, M.; Gil, M.; Dobkowski, J.; Wu, F.; Thummel, R. P.; Waluk, J. *Isr. J. Chem.* **1999**, *39*, 309. (c) Marks, D.; Zhang, H.; Borowicz, P.; Waluk, J.; Glasbeek, M., manuscript in preparation.
(38) del Valle, J. C.; Dominguez, E.; Kasha, M. *J. Phys. Chem. A* **1999**, *103*, 2467.
(39) Thummel, R. P.; Hegde, V. *J. Org. Chem.* **1989**, *54*, 1720.
(40) Wu, F.; Hardesty, J.; Thummel, V. *J. Org. Chem.* **1998**, *63*, 4055.
(41) Azawe, S. A.; Sarkis, G. Y. *J. Chem. Eng. Data* **1973**, *18*, 109.
(42) Naumenko, I. I.; Mikaleva, M. A.; Mamev, V. P. *Khim. Geterotsikl. Soedin*. **1981**, 958; *Chem. Heterocycl. Comput.* (English translation) **1982**, 710.

1.2 mmol) and polyphosphoric acid (PPA, 4.5 g) in toluene (20 mL) was refluxed for 2 h. After cooling, 15% NaOH solution (50 mL) was added until the solution was basic (pH = 10). The reaction mixture was extracted with $CH_2Cl_2$ (3 × 50 mL). The organic layers were combined, washed with brine, and dried over anhydrous $Na_2SO_4$. After the solvent was evaporated, the residue was purified by chromatography on alumina (15 g), eluting with $CH_2Cl_2$/hexane (2:1) to afford **DMPmIn-0** as a slightly yellow solid (165 mg, 59%): mp 120−121 °C; $^1$H NMR ($CDCl_3$) $\delta$ 9.58 (bs, 1H, NH), 7.68 (d, 1H, $J$ = 7.8 Hz, $H_4$), 7.43 (s, 1H, $H_{5'}$), 7.40 (d, 1H, $J$ = 8.4 Hz, $H_7$), 7.24 (t, 1H, $J$ = 7.5 Hz, H6), 7.11 (t, 1H, $J$ = 7.5 Hz, $H_5$), 6.84 (s, 1H, $H_3$), 2.50 (s, 6H, 4′- and 6′-$CH_3$); $^{13}$C NMR ($CDCl_3$) $\delta$ 166.7, 158.7, 136.8, 136.0, 128.9, 123.7, 121.9, 120.1, 117.7, 111.4, 104.6, 24.0.

The solvents were spectral grade and checked for the presence of fluorescing impurities. Absorption spectra were run on a Shimadzu UV3100 spectrophotometer. Steady-state fluorescence was recorded using an Edinburgh FS 900 CDT fluorometer (Edinburgh Analytical Instruments). Emission quantum yields were measured using quinine sulfate[43] ($\varphi_{fl}$ = 0.51) as a standard. Fluorescence decays were obtained on an Edinburgh FL 900 CDT time-resolved fluorometer (Edinburgh Analytical Instruments). The NOE NMR spectra were registered on a VARIAN UNITY PLUS 500 MHz spectrometer.

Structures and energies of both rotamers of **PyIn-0** were calulated by semiempirical (AM1[44]) and ab initio methods. In the latter, B3LYP and MP2 models were used, with 3-21G, 6-31G, 6-31G(d,p), and 6-31+G(d,p) basis sets, as implemented in the GAUSSIAN 98 suite of programs.[45] The Hessian matrix was analyzed in each case to ensure that the optimized geometry corresponds to a minimum on the potential energy surface. Ab initio optimized structures also served as input in molecular dynamics calculations. For the graphic presentation of results, gOpenMol[46] and Molden[47] software packages were used.

Classical molecular dynamics (MD) simulations are known to be a useful tool to provide a description of the influence of solvent effects on conformational equilibrium.[48−59] Studies of the systems of interest in different bulk solvent can provide information about the conformational preference caused by the medium effects. In the present study, the role of simulations was to elucidate how the intrinsic conformational preference can be altered by solute−solvent interactions. No attempt was made to analyze the dynamic aspects of solvation, since no corresponding experimental data are available at present.

**Table 1.** Lennard-Jones Parameters Used in Molecular Dynamics Calculations

| atom type | $\sigma$ (Å) | $\epsilon$ (kcal/mol) |
|---|---|---|
| C (aromatic) | 3.74 | 0.12 |
| N (pyridine) | 3.43 | 0.10 |
| N (pyrrole) | 3.43 | 0.09 |
| H (−C) | 2.37 | 0.03 |
| H (−N) | 0 | 0 |

**Solvent.** For the MD simulations in bulk solvent the chloroform[60] and methanol models were taken from the GROMOS96 solvent library. To mimic correctly the hydrogen-bonding properties of nitrogen and oxygen atoms, a special set of GROMOS96 van der Waals repulsion parameters was used. A solvent model of bulk *n*-hexane was adapted to the GROMOS96 force field from ref. 61. Although the bond lengths and angles were fixed as presented in ref 61, internal rotations around ordinary $CH_3-CH_2$ and $CH_2-CH_2$ bonds were also enabled, modeled with a standard GROMOS96 torsional potential energy function. The principal criterion for adjustment of force field parameters was the liquid density, which was reproduced as 0.68 ± 0.03 g/cm$^3$ (experimental value 0.66 g/cm$^3$) during an isothermal−isobaric MD simulation at 300 K and 1 atm.

**Solute.** The solute **PyIn-0** was represented by a rigid all-atom model with each atom considered a separate charge group. For this purpose, the standard GROMOS96 force field was modified using various semiempirical and ab initio levels of theory. At first, geometries of the *syn*- and *anti*-conformers were fully optimized by allowing all atoms to relax to a stationary point during the ab initio calculations carried out using the B3LYP model and 6-31+G(d,p) basis set. Parameters of the force field (bond lengths and angles) were adjusted to retain the ab initio geometry. The Lennard-Jones parameters, taken from the GROMOS96 force field without changes, are listed in Table 1. These parameters are known to describe quite well the nonbonded interactions in tryptophan-like molecules.[54−62] Atom-centered point charges used in modeling were taken from fits of the molecular electrostatic potential of the ground-state wave functions calculated at the same level of theory. These charges are very similar for the *syn*- and *anti*-conformers. For this reason, only the charges calculated for the *syn*-conformer were subsequently used. The aromatic rings in both rotamers were treated as rigid flat fragments, allowing the internal rotation around the central single bond linking the indole and pyridine moieties. A key issue underlying the reliability of the modeling of the *syn*−*anti* conformational equilibrium in **PyIn-0** is the need for a suitable torsional potential energy function that properly describes the interatomic interactions in modeled systems. This potential energy function was calculated by using the semiempirical AM1 Hamiltonian. Then, the standard GROMOS96 dihedral potential energy function expressed by eq 1

$$V(\Phi) = K_\theta [1 + \cos(\delta_n) \times \cos(n\Phi)] \quad (1)$$

($K_\theta$ = 8.37 kJ mol$^{-1}$, $\cos(\delta_n) = -1$, $n = 2$) was adjusted by fitting to the AM1 potential to reproduce the value of the energy barrier separating the *syn* and *anti* forms.

**Computational Protocol.** All simulations were performed with the GROMOS96 package of programs using the 43A1 force field.[63] The solute molecule was placed in the center of a cubic box, which was filled with the appropriate solvent at an equilibrium distribution. Solvent

(43) Velapoldi, R. A. *Natl. Bur. Stand. 378, Proc. Conf. NBS*; Gaithersburg 1972, 231.
(44) Dewar, M. J. S.; Zoebisch, E. G.; Healy, E. F.; Stewart, J. J. P. *J. Am. Chem. Soc.* **1985**, *107*, 3902.
(45) Frisch, M. J.; Trucks, G. W.; Schlegel, H. B.; Scuseria, G. E.; Robb, M. A.; Cheeseman, J. R.; Zakrzewski, V. G.; Montgomery, J. A., Jr.; Stratmann, R. E.; Burant, J. C.; Dapprich, S.; Millam, J. M.; Daniels, A. D.; Kudin, K. N.; Strain, M. C.; Farkas, O.; Tomasi, J.; Barone, V.; Cossi, M.; Cammi, R.; Mennucci, B.; Pomelli, C.; Adamo, C. Clifford, S.; Ochterski, J.; Petersson, G. A.; Ayala, P. Y.; Cui, Q.; Morokuma, K.; Malick, D. K.; Rabuck, A. D.; Raghavachari, K.; Foresman, J. B.; Cioslowski, J.; Ortiz, J. V.; Stefanov, B. B.; Liu, G.; Liashenko, A.; Piskorz, P.; Komaromi, I.; Gomperts, R.; Martin, R. L.; Fox, D. J.; Keith, T.; Al-Laham, M. A.; Peng, C. Y.; Nanayakkara, A.; Gonzalez, C.; Challacombe, M.; Gill, P. M. W.; Johnson, B.; Chen, W.; Wong, M. W.; Andres, J. L.; Gonzalez, C.; Head-Gordon, M.; Replogle, E. S.; Pople, J. A. *Gaussian 98*, revision A.6; Gaussian, Inc.: Pittsburgh, PA, 1998.
(46) Laaksonen, L. *gOpenMol*, version 1.3; Centre for Scientific Computing: Espoo, Finland, 1997.
(47) Schaftenaar, G. *MOLDEN: A Portable Electron Density Program*; *QCPE Bull.* **1992**, *12*, 3.
(48) Jorgensen, W. L. *J. Phys. Chem.* **1983**, *87*, 5304.
(49) Mark, A. E.; Berendsen, H. J. C.; van Gunsteren, W. F. *Biochemistry* **1991**, *30*, 10866.
(50) Nilsson, J. A.; Laaksonen, A.; Eriksson, L. A. *J. Chem. Phys.* **1998**, *109*, 2403.
(51) Daura, X.; Gademan, K.; Jaun, B.; Seebach, D.; van Gunsteren, W. F.; Mark, A. E. *Angew. Chem., Int. Ed.* **1999**, *38*, 236.
(52) Tayar, N. E.; Mark, A. E.; Vallat, P.; Brunne, R. M.; Testa, B.; van Gunsteren, W. F. *J. Med. Chem.* **1993**, *36*, 3757.
(53) Ahlstrom, P.; Berendsen, H. J. C. *J. Phys. Chem.* **1993**, *97*, 13691.
(54) Daura, X.; Suter, R.; van Gunsteren, W. F. *J. Chem. Phys.* **1999**, *110*, 3049.
(55) Liu, H.; Müller-Plathe, F.; van Gunsteren, W. F. *J. Chem. Phys.* **1995**, *102*, 1722.
(56) Beutler, T. C.; van Gunsteren, W. F. *J. Chem. Phys.* **1994**, *100*, 1492.
(57) Bonanno, G.; Noto, R.; Fornii, S. L. *J. Chem. Soc., Faraday Trans.* **1998**, *94*, 2755.
(58) Chipot, C.; Pohorille, A. *J. Phys. Chem.* B, **1998**, *102*, 281.
(59) Worth, G. A.; Nardi, F.; Wade, R. C. *J. Phys. Chem.* B, **1998**, *102*, 6260.
(60) Tironi I. G.; van Gunsteren W. F. *Mol. Phys.* **1994**, *83*, 381.
(61) Jorgensen, W. L.; Modura, J. D.; Carol J. S. *J. Am. Chem. Soc.* **1984**, *106*, 6638.
(62) Daura, X.; Hunenberger, P. H.; Mark, A. E.; Querol, E.; Aviles, F. X.; van Gunsteren, W. F. *J. Am. Chem. Soc.* **1996**, *118*, 6285.
(63) Scott, W. R. P.; Hünenberger, P. H.; Tironi, I. G.; Mark, A. E.; Billeter, S. R.; Fennen, J.; Torda, A. E.; Huber, T.; Krüger, P.; van Gunsteren, W. F. *J. Phys. Chem. A* **1999**, *103*, 3596.

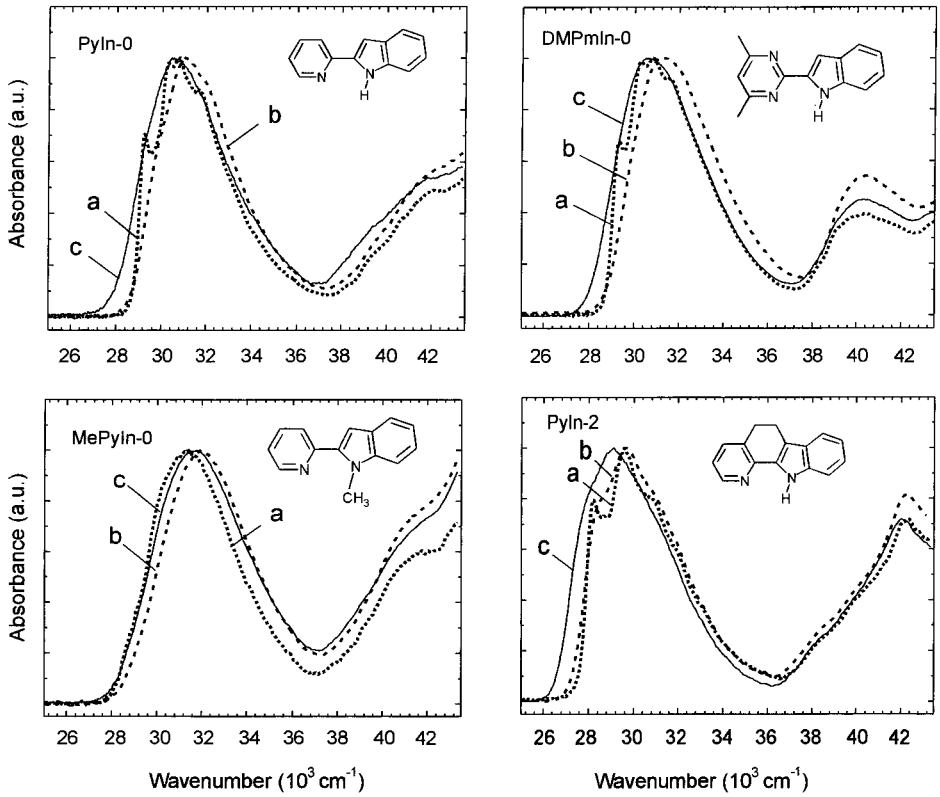


**Figure 1.** Room-temperature electronic absorption spectra in (a) *n*-hexane (dotted line), (b) acetonitrile (dashed line), and (c) 1-propanol (solid line). Top left, **PyIn-0**; bottom left, **MePyIn-0**; top right, **DMPmIn-0**; bottom right, **PyIn-2.**

molecules lying outside the box or overlapping with solute atoms (solute−solvent distance < 0.23 Å) were removed. The final systems included 310, 216, and 462 solvent molecules for *n*-hexane, chloroform, and methanol, respectively. Each system was first energy-minimized to obtain the starting structure for molecular dynamic simulations. For solvent equilibration 50 ps were then allowed at constant temperature and volume, followed by another 50 ps at constant temperature and pressure. Subsequently, the whole system was allowed to relax for 100 ps, after which the trajectories were collected for 700 ps. The trajectories were saved every 10 fs. All simulations were performed using a periodic boundary condition at a temperature of 300 K and a pressure of 1 atm. The temperature and the pressure were maintained by weak coupling to an external bath,[64] using a relaxation time of 0.1 and 0.5 ps, respectively. The bond lengths were constrained using the SHAKE algorithm[65] with geometry tolerance of $10^{-4}$. The integration time step was 0.5 fs. A cutoff radius of 1.1 Å was used for nonbonded interactions. The nonbonded interactions were calculated at each time step using a charge-group pair list that was updated every 20 time steps.

## Results and Discussion

Electronic absorption spectra of **PyIn-0**, **MePyIn-0**, **PyIn-2**, **3′-PyIn-0**, **4′-PyIn-0,** and **DMPmIn-0** are compared in Figures 1 and 2. Upon passing from a nonpolar to a polar aprotic solvent, the first absorption band reveals a loss of vibronic structure and a slight blue shift. In protic solvents, a red shift is observed, pointing to a specific hydrogen-bond interaction. This behavior is characteristic for all the molecules investigated except **MePyIn-0**, the only indole that lacks the NH group. The spectral changes in alcohols are associated with the formation of an intermolecular hydrogen bond, in which the alcohol molecule accepts a proton from the NH group. This finding is in line with our earlier observation that adding species which can only act as proton acceptors (e.g., DMSO) to aprotic solutions of pyridylindoles produces spectral changes similar to those caused by alcohols.[34]

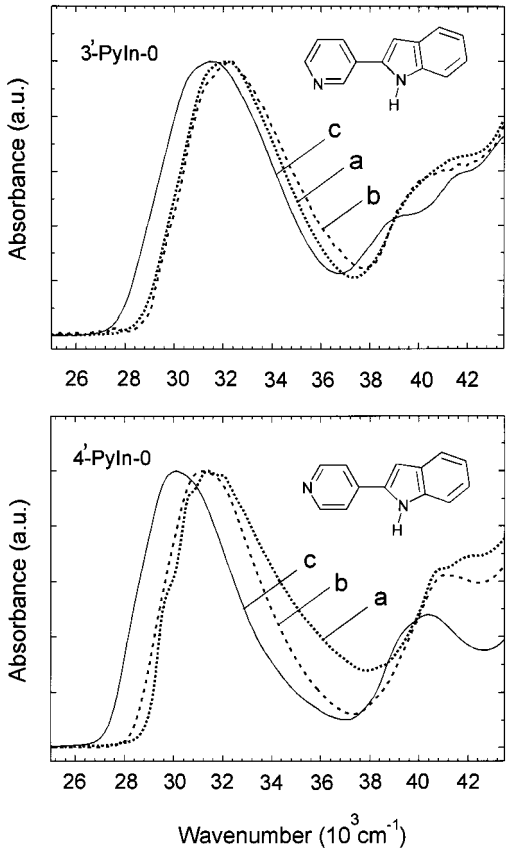


**Figure 2.** Room-temperature electronic absorption spectra: Top, **3′-PyIn-0**; bottom, **4′-PyIn-0**. See caption to Figure 1 for details.

(64) Berendsen, H. J. C.; Pastma, J. P. M.; van Gunsteren, W. F., Nola, A., Haak, J. R. *J. Chem. Phys.* **1984**, *81*, 3684.

(65) Ryckaert J. P., Ciccott, G.; Berendsen, H. J. C. *J. Comput. Phys.* **1977**, *23*, 327.

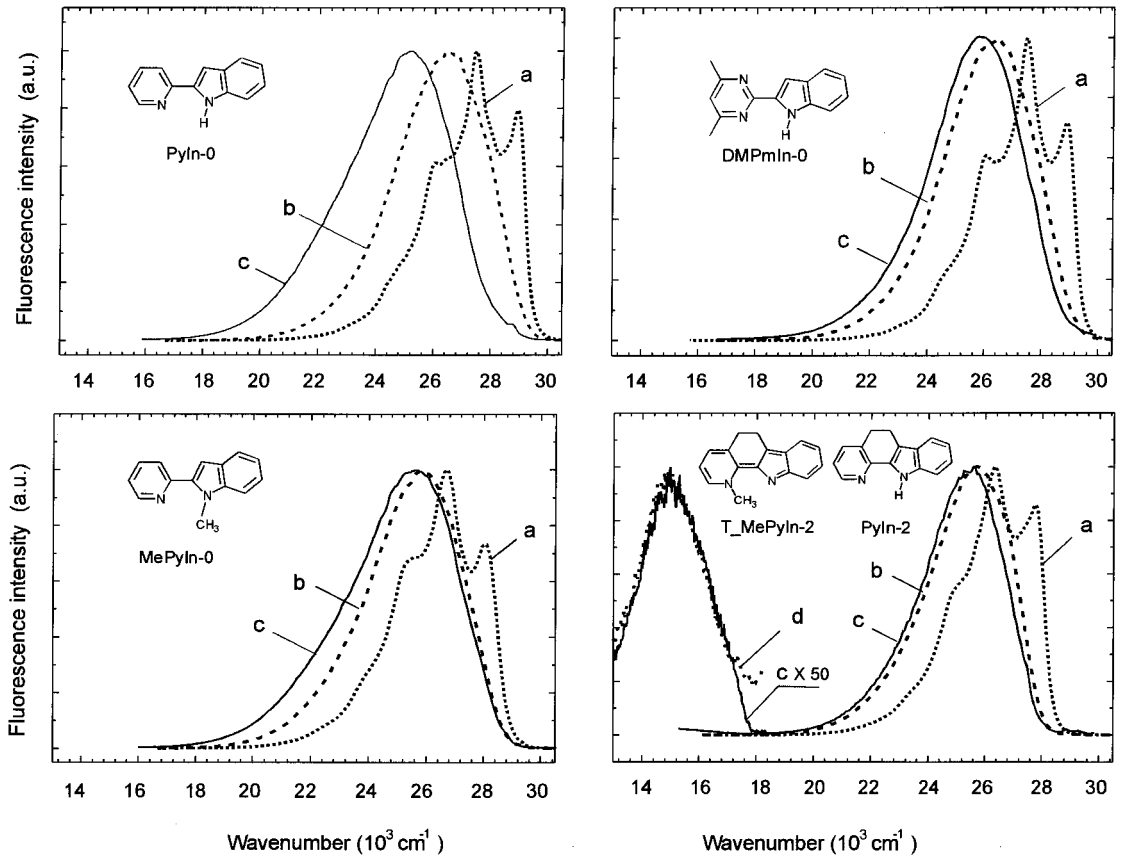


**Figure 3.** Room-temperature fluorescence spectra: Top left, **PyIn-0**; bottom left, **MePyIn-0**; top right, **DMPmIn-0**; bottom right, **PyIn-2** and **T_MePyIn-2** (d, measured in 1-propanol). See caption to Figure 1 for details.

The absorption curves of **PyIn-0** and **DMPmIn-0** are very similar. At first glance, this result is not obvious, since the latter molecule has one more hydrogen-bonding center than the former. However, as will be shown below, the hydrogen-bonding pattern of **DMPmIn-0** corresponds to that of the mixture of *syn* and *anti* rotamers of **PyIn-0**.

Figure 3 presents the fluorescence spectra of **PyIn-0** in different solvents, compared with the analogous data for **MePyIn-0**, **DMPmIn-0** and the bridged derivative, **PyIn-2**. Emission spectra of **3′-PyIn-0** and **4′-PyIn-0** are shown in Figure 4. Table 2 contains relevant photophysical parameters.

The largest differences in photophysical behavior are observed in alcohol solutions. In all compounds except **4′-PyIn-0**, the emission in alcohols is weaker than in aprotic solvents, both polar and nonpolar. However, while the quenching of fluorescence in alcohols is very strong in **PyIn-2** (and other bridged 2-(2′-pyridyl)indoles[32,34]) as well as in **DMPmIn-0**, **PyIn-0** and **MePyIn-0** reveal a much smaller decrease in quantum yield. It is instructive to compare the fluorescence efficiencies of **PyIn-0** and the bridged derivatives with the quantum yields measured in another hydrogen-bonding solvent, pyridine, which was also found to quench the emission. For the bridged compounds, the quantum yields in pyridine are higher than those in alcohols, while the opposite is true for **PyIn-0**.[33] Also, the position of fluorescence maxima in alcohols and pyridine are not the same in **PyIn-0**, whereas they were found to coincide in all four bridged pyridylindoles, **MePyIn-0**, as well as in the N-methylated derivative of **PyIn-2**.

Contrary to the case of absorption, no similarity is found in the emission pattern of **PyIn-0** and **DMPmIn-0**. A considerable red shift, observed in the former upon passing from a polar aprotic acetonitrile to a polar protic alcohol, is not reproduced in the latter.

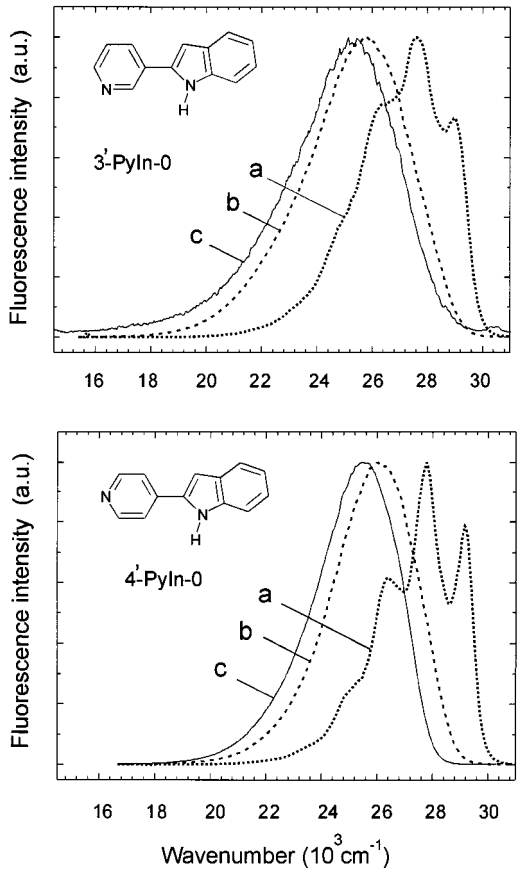


**Figure 4.** Room-temperature fluorescence spectra: Top, **3′-PyIn-0**; bottom, **4′-PyIn-0**. See caption to Figure 1 for details.

**Table 2.** Photophysical Parameters Measured at 298 K

| solvent | $\nu_{abs}$[a] [$10^3$cm$^{-1}$] | $\nu_{fl}$[b] [$10^3$cm$^{-1}$] | $\phi_{fl}$[c] | $\tau_{fl}$[d] [ns] | $k_r \times 10^7$ [e] [s$^{-1}$] | $k_{nr} \times 10^9$ [f] [s$^{-1}$] |
|---|---|---|---|---|---|---|
| | | | **PyIn-0** | | | |
| *n*-hexane | 30.80 | 27.50 | 0.48 | 1.3 | 38.4 | 0.42 |
| acetonitrile | 31.00 | 26.45 | 0.53 | 1.8 | 30.3 | 0.27 |
| 1-propanol | 30.40 | 24.60 | 0.11 | 3.2($\tau_1$)[g]<br><0.2($\tau_2$)[g] | | |
| | | | **MePyIn-0** | | | |
| *n*-hexane | 31.40 | 26.80 | 0.51 | 1.9 | 27.1 | 0.26 |
| acetonitrile | 31.95 | 25.80 | 0.61 | 2.5 | 24.4 | 0.16 |
| 1-propanol | 31.70 | 25.30 | 0.09 | 0.6 | 16.3 | 1.65 |
| | | | **3′-PyIn-0** | | | |
| *n*-hexane | 31.40 | 27.50 | 0.99 | 2.0 | 49.5 | 0.005 |
| acetonitrile | 32.00 | 25.80 | 0.98 | 3.4 | 28.8 | 0.006 |
| 1-propanol | 31.30 | 25.25 | 0.05 | ≤0.4 | ≥12.5 | ≥2.4 |
| | | | **4′-PyIn-0** | | | |
| *n*-hexane | 32.20 | 27.75 | 0.83 | 1.6 | 52.0 | 0.1 |
| acetonitrile | 31.10 | 26.00 | 0.88 | 3.0 | 29.5 | 0.04 |
| 1-propanol | 30.00 | 25.55 | 0.73 | 2.7 | 27.1 | 0.1 |
| | | | **DMPmIn-0** | | | |
| *n*-hexane | 30.85 | 27.45 | 0.62 | 1.7 | 36.5 | 0.2 |
| acetonitrile | 31.30 | 26.30 | 0.70 | 2.4 | 29.1 | 0.1 |
| 1-propanol | 30.50 | 25.80 | 0.02 | <0.3 | >6.7 | >3.3 |
| | | | **PyIn-2** | | | |
| *n*-hexane | 29.60 | 26.35 | 0.50 | 1.3 | 38.5 | 0.4 |
| acetonitrile | 29.65 | 25.70 | 0.38 | 1.8 | 21.1 | 0.3 |
| 1-propanol $F_1$ | 29.05 | 25.50 | 0.006 | <0.2 | >3.0 | >4.9 |
| $F_2$ | | 14.90 | 0.0004 | <0.2 | >0.2 | >5.0 |

[a] The maximum of the first absorption band. [b] Fluorescence maximum. [c] Fluorescence quantum yield, accuracy: ±20%. [d] Fluorescence lifetime. [e] The radiative constant of $S_1 \rightarrow S_0$ depopulation. [f] Sum of the nonradiative constants of $S_1$ depopulation. [g] Biexponential decay

These results lead to two conclusions. First, the mechanism of fluorescence quenching by alcohols, very efficient in bridged pyridylindoles, remains effective in **DMPmIn-0**, but seems much less important in **PyIn-0**, while in **4′-PyIn-0** it does not operate at all. Second, the fluorescence of **PyIn-0** in alcohols may have a different origin than the emission of the same compound in other solvents, including protic hydrogen-bond acceptors, such as pyridine.

Our previous work on fluorescence quenching in pyridylindoles has shown that the origin of the quenching lies in the capability of forming complexes with alcohol molecules.[32−37] Other possible channels of excited-state deactivation, such as out-of-plane motion or $^1L_b-{}^1L_a$ states inversion could be excluded, on the basis of (i) comparison of the properties of pyridylindoles with those of 2-phenylindole; (ii) measurements of the same chromophore in nonpolar and polar aprotic solvents, and (iii) studies of various chromophores with different $^1L_a-{}^1L_b$ separations. It was established that the deactivation of the lowest excited singlet state in such species can include two channels not available in aprotic solvents: (1) excited state double proton transfer, occurring in cyclic, doubly hydrogen-bonded complexes; (2) rapid $S_1 \rightarrow S_0$ internal conversion, again observed only in compounds for which the topology enables the formation of cyclic solvates.

The present results corroborate the above model and can be explained on its basis. We interpret the lack of fluorescence quenching in alcohol solutions of **4′-PyIn-0** as due to the geometry of the molecule which is inappropriate for the formation of cyclic complexes with alcohols. However, **DMPmIn-0** can form such cyclic complexes, and therefore, its emission is efficiently quenched. The most interesting and somewhat unexpected result is obtained for **PyIn-0**. Its behavior can be understood provided that only a fraction of the molecules exists in alcohols as *syn* rotamers, the form capable of forming cyclic solvates. The other fraction, dominant in alcohols, should exists as *anti* rotamers which are unable to form such complexes.

The presence of two different forms of **PyIn-0** in alcohols was confirmed by time-resolved fluorescence measurements. The fluorescence decays, measured in aprotic solvents, both polar and nonpolar, were monoexponential. In alcohols, however, biexponential decays were obtained (Table 2). One of the decay times was too short (<200 ps) at room temperature to be determined accurately. The other component was longer than the monoexponential decay time observed in aprotic solvents. Lowering of the temperature influenced the two decays in a different fashion. The decay time corresponding to the longer component increased only about two times, while the decay time corresponding to the shorter one was getting much slower, approaching a value similar to that obtained in aprotic media.

An obvious interpretation of the results obtained for alcohol solutions is the assignment of the shorter decay to the *syn* conformer, of which the lowest excited singlet state is rapidly deactivated at room temperature. We have previously shown that lowering the temperature leads to the recovery of the radiative properties in alcohol solutions. The activation energy of the quenching process was found to correlate with the activation energy of the solvent viscous flow.[34] The present results are in accordance with this observation. For instance, in 1-butanol, the decay time of the *syn* rotamer at 214 K is about 2 ns, while in 1-propanol, less viscous at this temperature, the corresponding value is 1.4 ns.

From the values of the lifetimes and relative amplitudes, the ratio of the *syn* to *anti* rotamers was estimated as approximately 1:4. Using this ratio and the measured quantum yields and lifetimes of fluorescence, the value of $(4/5) \times 10^7$ s$^{-1}$ was obtained for the rate of radiative depopulation of $S_1$ in the *anti* form. This value is somewhat smaller than that estimated for the *syn* rotamer, $(2/3) \times 10^8$ s$^{-1}$. Judging by comparable fluorescence lifetimes of the *syn* form at low temperatures in both protic and aprotic solvents, this constant is similar in the *syn* complex with alcohol and in the uncomplexed molecule.

**Table 3.** Calculated Energy Differences (kcal/mol) between *syn* and *anti* Rotamers

| | PyIn-0 | MePyIn-0 | 3′-PyIn-0 |
|---|---|---|---|
| B3LYP/3-21G[a] | −4.40 | −3.33 | −0.27 |
| B3LYP/6-31G[a] | −4.49 | −3.02 | −0.34 |
| B3LYP/6-31G(d,p)[a] | −4.53 | −2.64 | −0.26 |
| MP2/6-31G+(d,p)// B3LYP/6-31G(d,p)[b] | −4.32 | −2.30 | −0.06 |

[a] $\Delta E = E(\text{B3LYP})_{syn} - E(\text{B3LYP})_{anti}$. [b] $\Delta E = E(\text{MP2//B3LYP})_{syn} - E(\text{MP2//B3LYP})_{anti} + (\text{ZPE(B3LYP})_{syn}\text{-ZPE(B3LYP})_{anti}) \times 0.96$ (scale factor from ref 66).

Final arguments for the assignment of the *syn* and *anti* rotamers were provided by NOE experiments. The proton NMR spectra of **PyIn-0** were recorded in aprotic $CDCl_3$ and hydrogen-bonding MeOD. The relative intensities were compared for the signals corresponding to two pairs of protons: $H_3-H_{3'}$ and $H_{5'}-H_{6'}$, where the primed symbols refer to positions in the pyridyl ring (see Chart 1). While the latter signal intensities are not expected to be very different in *syn* and *anti* rotamers, the former signal intensities should greatly diminish in the *anti* form, due to a much larger distance between $H_3$ and $H_{3'}$ protons. Upon going from chloroform to methanol, the ratio of the two signals decreased about 6-fold due to the *anti* form being dominant in methanol. Since only *syn* species are present in chloroform (no longer fluorescence lifetime, corresponding to the *anti* form was observed), we find that about 85% of the ground-state population in alcohol corresponds to the *anti* rotamers. This estimate is in excellent agreement with the value of 80% obtained from fluorescence decay measurements. Since the latter value refers to the excited-state population, these results indicate that there is no interconversion between the rotamers in the excited state. On the other hand, the interconversion in the ground state, faster than the NMR time scale, is evidenced by the lack of separate NMR signals for each of the two forms.

The reason for the reversal of the relative stabilities of the *syn* and *anti* rotamers of **PyIn-0** in alcohols must be due to the stabilization of the latter by hydrogen bonding to the solvent. The effect due to different stabilization of the two forms in polar solvents should be rather small, as the computed ground-state dipole moments are very similar (2.44 D vs. 3.44 D for *syn* and *anti* rotamers, respectively, calculated using B3LYP/6-31+G(d,p)). Calculations performed for the two forms of the isolated molecule predict that the *syn* structure should be more stable by about 4.3 kcal/mol (Table 3). Apparently, hydrogen-bond formation can compensate for this difference. Several observations indicate that the stable *anti* rotamer actually corresponds to a 1:2 complex with alcohol. When studying changes in fluorescence behavior upon addition of alcohol to a solution of **PyIn-0** in a nonpolar solvent, we observed the appearance of a longer decay time, attributed to the *anti* form only at high alcohol concentrations. Moreover, the fluorescence quantum yield, measured as a function of alcohol concentration, revealed a minimum at $C_{alc} \approx 1$ M. These findings suggest that the 1:1 complexes of the *syn* form with alcohol are formed first. Only when the alcohol concentration is high enough, are the 1:2 complexes produced, and thus the *syn* → *anti* transformation occurs. The 1:2 structure of the *anti* rotamer is also in accordance with the observation that no *anti* form was found in **MePyIn-0**, a molecule which can only form one hydrogen bond. Both the fluorescence quantum yield and lifetime of **MePyIn-0** decrease by the same amount in alcohol solutions, revealing a very similar radiative constant, and thus, probably the same *syn* structure as in aprotic solvents. This result is interesting also because calculations for **MePyIn-0** predict a smaller energy difference between the two rotamers than for **PyIn-0** (Table 3).

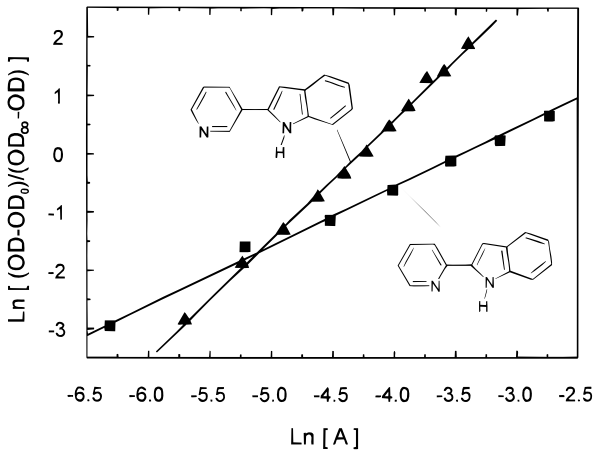


**Figure 5.** Determination of the stoichiometry of 1-butanol solvates. The number of alcohol molecules in the complex, *n*, is given by the slope of the plot. Absorbance changes were monitored at 350 nm (**PyIn-0**) and at 344 nm (**3′-PyIn-0**). For **PyIn-0** (squares), $n = 1.02 \pm 0.06$, correlation coefficient $r = 0.998$. For **3′-PyIn-0** (triangles), $n = 2.06 \pm 0.06$, correlation coefficient $r = 0.999$.

Thus, the behavior of **PyIn-0** in bulk alcohols can be described by two equilibria:

$$\textbf{PyIn-0} + \text{A} \rightleftharpoons \text{C}_{11}$$

$$K_{11} = [\text{C}_{11}]/([\text{A}][\textbf{PyIn-0}])$$

$$\text{C}_{11} + \text{A} \rightleftharpoons \text{C}_{12}$$

$$K_{12} = [\text{C}_{12}]/([\text{A}]^2[\textbf{PyIn-0}])$$

where A denotes an alcohol molecule, while $C_{11}$ and $C_{12}$ correspond to 1:1 and 1:2 complexes, respectively. It follows that $[C_{12}]/[C_{11}] = [A]K_{12}/K_{11}$. From the analysis of the titration curves of **PyIn-0** in *n*-hexane with 1-butanol (Figure 5), a value of $K_{11} = 28\ \text{M}^{-1}$ was obtained at 293 K. Temperature dependence of the $K_{11}$ value yielded $\Delta H = -6.2 \pm 0.5$ kcal/mol, and $\Delta S = -17.8 \pm 1.5$ eu. Recalling that $C_{21}$:$C_{11} \approx 4$ in bulk alcohols, we obtain $K_{12} \approx 10.3\ \text{M}^{-2}$. These values imply that in mixed solvents the 1:2 complexes will start to dominate over the 1:1 solvates only at high alcohol concentrations ($C_{21}$:$C_{11} \geq 1$ at [A] ≥ 2.7 M).

The titration was performed at alcohol concentrations low enough to ensure that no dimers or higher oligomers of alcohol are formed (0.002 M < [A] < 0.02 M). The value of the slope of the plot of $\ln[(\text{OD} - \text{OD}_0)/(\text{OD}_\infty - \text{OD})]$ vs ln[A] (Figure 5), $n = 1.02 \pm 0.06$ indicates that most of the **PyIn-0** complexes formed at this alcohol concentration have a 1:1 stoichiometry. In contrast, a value of $n = 2.06 \pm 0.06$ is obtained for **3′-PyIn-0** in the same alcohol concentration range. Several reasons for this difference between these two isomers can be suggested. The two hydrogen-bonding centers in **3′-PyIn-0** are further apart than in **PyIn-0**. Therefore, steric factors do not inhibit formation of two hydrogen bonds with two different alcohol molecules in both the *syn* and *anti* conformers of **3′-PyIn-0**. Actually, calculations predict that the *syn* and *anti* rotamers of **3′-PyIn-0** have similar energies (Table 3), so both forms should be present even in nonpolar aprotic solvents**.** However, fluorescence lifetime measurements reveal single exponential decays, which points to the presence of only one rotamer. It is particularly interesting to find that the fluorescence of **3′-PyIn-0** is quenched in alcohols (Table 2). We tentatively postulate that the quenching

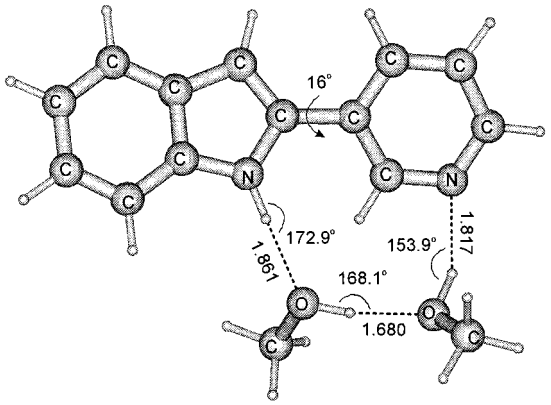


**Figure 6.** The structure of a 1:2 complex between **3′-PyIn-0** and methanol (B3LYP/6-31G calculation).

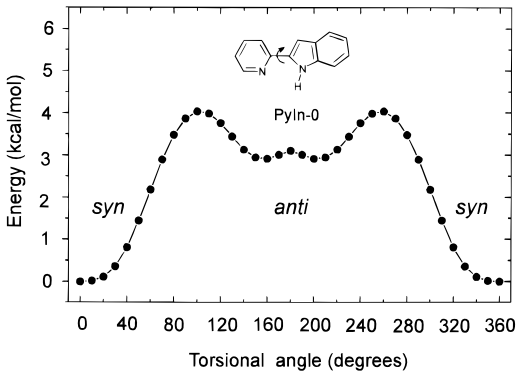


**Figure 7.** The potential for *syn*−*anti* isomerization of **PyIn-0** as a function of the dihedral angle between the indole and pyridine planes, calculated by the AM1 method. See text for discussion.

may be caused by the formation of a cyclic solvate of 1:2 stoichiometry, the calculated structure of which is shown in Figure 6. Proton transfer in the complex could be the reason for enhanced depopulation of the lowest excited singlet state. Similar solvate structure has been observed for 7-hydroxyquinoline, where excited-state proton-transfer according to a "proton relay" mechanism has been proposed.[67]

Initial attempts to interpret the *syn*−*anti* isomerism of **PyIn-0** in alcohol by comparing calculated energies of alcohol complexes for both rotamers were not successful. No distinct stabilization was obtained for the 1:2 complexes of the *anti* form. It seems more probable that the phenomenon is caused by collective effects due to both, specific interaction (i.e., hydrogen bonding) and nonspecific solvation by alcohol. Therefore, we decided to determine whether the conformational change in alcohols may be reproduced by molecular dynamics calculations. The computations used the AM1 calculated potential for *syn*−*anti* isomerism presented in Figure 7 and the atomic charges given in Figure 8. The distributions of the dihedral angle between the pyridine and indole planes, calculated for three

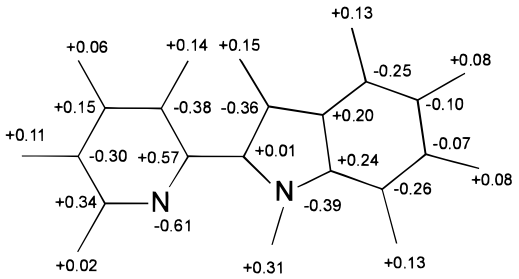


**Figure 8.** Atomic charges obtained by B3LYP/6-31+G(d,p) ab initio calculations, used in the input for molecular dynamics simulations.

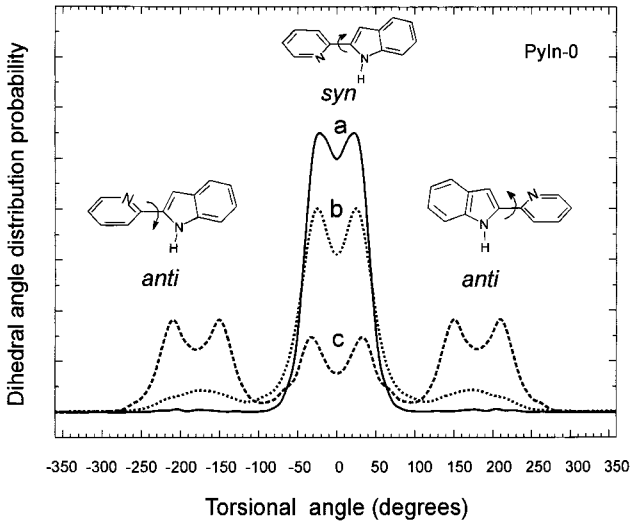


**Figure 9.** Distributions of the dihedral angles between the pyridine and indole planes in **PyIn-0** obtained by molecular dynamics for three different solvents: (a) *n*-hexane, (b) chloroform, and (c) methanol.

different solvents, are shown in Figure 9. It is natural to define the *syn* conformers as those for which the value of the dihedral angle between the indole and pyridine planes varies between $-\pi/2$ and $\pi/2$. Using this definition, the calculated fractions of the *anti* conformer are 2, 20, and 70% for *n*-hexane, chloroform, and methanol, respectively. While the quantitative agreement with experiment obtained for *n*-hexane and alcohol is probably fortuitous, given the approximate form of the potential governing the rotamerization, these results clearly show the potential of molecular dynamics for studying conformational equilibria in condensed phase. We plan to pursue this type of investigation using more accurate potentials and comparing the results obtained for isomeric molecules—for instance **PyIn-0** and 2-(2′-quinolylo)pyrrole. Initial results for the latter also point to the presence of two rotamers in alcohol.

Both quantum chemical and molecular dynamics calculations predict that the structure of 1:1 complexes in the *syn* form corresponds to a cyclic species. Our experimental results, however, suggest that this may be the case only in mixtures of aprotic solvents with small amounts of alcohol, but not in bulk alcohols. The recovery of the radiative properties of **PyIn-0** at low temperatures in alcohol glasses means that the complexes are not capable of undergoing excited-state double proton transfer under these conditions. On the contrary, the phototautomerization has been observed in rigid alcohol solutions of **DPC**, **TPC**, and **PQ** and interpreted as evidence of the presence of cyclic species even at low temperatures.[36,37] Another argument is the lack of tautomeric emission in **PyIn-0**. As discussed above, two competing channels, proton transfer and internal conversion to the ground state, are responsible for the fast depopulation of the lowest excited singlet state of the 1:1 alcohol

(66) (a) Curtiss, L. A.; Raghavachari, K.; Redfern, P. C.; Pople, J. A. *Chem. Phys. Lett.* **1997**, *270*, 419. (b) El-Azhary, A. A.; Suter, H. U. *J. Phys. Chem.* **1996**, *110*, 15056.

(67) (a) Itoh, M.; Adachi, T.; Tokumura, K. *J. Am. Chem. Soc.* **1983**, *105*, 4828; *ibid.* **1984**, *106*, 850. (b) Nakagawa, T.; Kohtani, S.; Itoh, M. *J. Am. Chem. Soc.* **1995**, *117*, 7952. (c) Tokumura, K.; Natsume, M.; Nakagawa, T.; Hashimoto, M.; Yuzawa, T.; Hamaguchi, H.; Itoh, M. *Chem. Phys. Lett.* **1997**, *271*, 320. (d) Kang, W. K.; Cho, J. S.; Lee, M.; Kim, D. H.; Ryoo, R.; Jung, K. H.; Jang, D. J. *Bull. Korean Chem. Soc.* **1992**, *13*, 140. (e) Lee, S.-I.; Jang, D.-J. *J. Phys. Chem.* **1995**, *99*, 7537. (f) Lavin, A.; Collins, S. *Chem. Phys. Lett.* **1993**, *204*, 96; *ibid.* **1993**, *207*, 513; Bohra, A.; Lavin, A.; Collins, S. *J. Phys. Chem.* **1994**, *98*, 11427. (g) Konijnenberg, J.; Ekelmans, G. B.; Huizer, A. H.; Varma, C. A. G. O. *J. Chem. Soc. Faraday Trans. 2* **1989**, *85*, 39.

**Table 4.** Changes of p$K_a$ upon $S_1 \leftarrow S_0$ Excitation, Calculated Using the Förster Cycle[68]

| | $\Delta pK_a$ |
|---|---|
| **PyIn-0** | 11.1 ± 1.0 |
| **MePyIn-0** | 10.5 ± 1.0 |
| **3′-PyIn-0** | 12.6 ± 2.5 |
| **4′-PyIn-0** | 12.1 ± 1.0 |
| **PyIn-2** | 12.2 ± 2.5 |

complexes of the *syn* species. The phototautomerization is favored in cyclic species, while noncyclic complexes are most readily deactivated via internal conversion. The latter seems to be the dominant channel in bridged pyridylindoles,[34,37] although an extremely weak tautomeric emission is also detected (Figure 3). Lack of such emission in **PyIn-0** and **DMPmIn-0** indicates that the internal conversion process is dominant in these compounds, and thus, that their complexes with alcohol are not cyclic. We cannot, however, totally exclude another possibility, a very low emission yield for the tautomer of these two compounds. In fact, our efforts to register fluorescence of **T_MePyIn-0**, a model of the **PyIn-0** tautomer, failed, while for **T_MePyIn-2**, a model of **PyIn-2** tautomer, such emission was observed (Figure 3).

Finally, one should also mention the possibility of yet another channel for deactivation — excited-state protonation on the pyridine nitrogen. Thermodynamically, such a process is very favorable, since p$K_a$ changes upon $S_0 \rightarrow S_1$ excitation are very large (Table 4). However, measurements performed for the protonated species reveal weak fluorescence in the region 18 000−19 000 $cm^{-1}$ and since no such emission is observed in alcohol solutions, we exclude protonation in $S_1$ as a main source of fluorescence quenching.

On the other hand, excited-state protonation was detected in water. Fluorescence of the monocation appeared even when only the neutral form was observed in absorption. Therefore, the studies of possible rotamerization in water had to be performed in alkaline solutions. Under these conditions, no evidence for rotamerization was found. Very similar, low-intensity fluorescence, with a maximum around 23 000 ±1000 $cm^{-1}$ was observed both for bridged and unbridged pyridylindoles. The measured decay times were very short. In particular, no longer lifetime, characteristic of the *anti* form was detected for **PyIn-0**. While the assignment of the emission in water is not yet clear (it may be due to the anion or an exciplex), it is obvious that no rotamerization occurs in bulk alkaline water solutions.

However, the process was observed for **PyIn-0** solutions in acetonitrile, to which small amounts of water were being added. Figure 10 compares the results of titration with water of the acetonitrile solutions of **PyIn-0** and **PyIn-2**. Fluorescence quenching is observed in both cases. However, in the case of **PyIn-0** it is accompanied by a considerable red shift of the emission, while in **PyIn-2** (and also in **4′-PyIn-0**) the shift is much smaller (Figure 11). Moreover, the quenching is much stronger for **PyIn-2**. In **PyIn-0**, the fluorescence quantum yield goes through a minimum for water concentration around $10^{-3}$ M, and then slightly rises (Figure 12). Such minimum, analogous to that found for the titration of *n*-hexane solutions of **PyIn-0** with alcohols, is indicative of the appearance of another form with a higher fluorescence quantum yield. The *anti* form is an obvious candidate. The decisive arguments were provided by fluorescence decay measurements. For **PyIn-2**, only a single decay time was detected, which decreased upon addition of water. On the contrary, upon addition of water to acetonitrile solutions of **PyIn-0**, double-exponential decay was observed, consisting of a short (a few picoseconds) and a long (about 5 ns) component. The latter started to dominate at water concentrations similar to those for which the minimum of fluorescence intensity was observed. These results are in perfect analogy to the observations obtained for **PyIn-0** in mixtures of nonpolar solvents with alcohols. Therefore, we conclude that specific hydrogen-bonding interactions with water, when the latter is dispersed in other solvent can cause, as in the case of alcohols, the *syn* → *anti* transformation of **PyIn-0**.

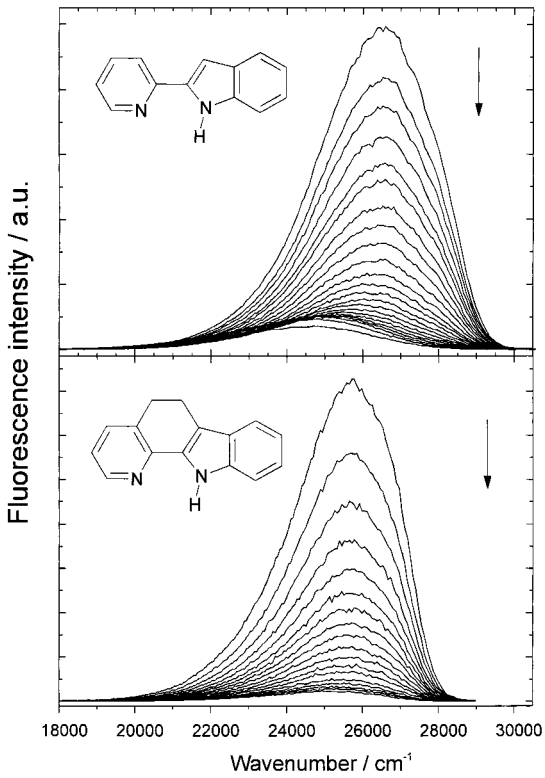


**Figure 10.** Fluorescence changes occurring during titration of acetonitrile solutions of **PyIn-0** (top) and **PyIn-2** (bottom) with water at 293 K. The arrows indicate increasing water content. The water concentration ranged from 0 to $1.759 \times 10^{-2}$ M. See Figures 11 and 12 for exact analysis of fluorescence shifts and quantum yields as functions of concentration.

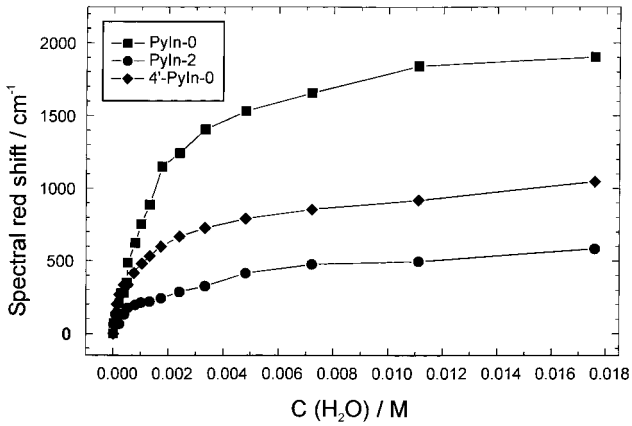


**Figure 11.** Spectral shifts of the fluorescence maxima accompanying titration of acetonitrile solutions of **PyIn-0**, **4′-PyIn-0** and **PyIn-2** with water at 293 K.

It may be instructive in this context to recall that the presence of tautomeric fluorescence in water solutions of 7-azaindole is still under debate[24,29] (while in alcohol solutions this emission is readily detected). However, this emission can be induced in water upon addition of ethyl ether or DMSO. This, according to Chou et al.,[28] leads to the disruption of water clusters and to

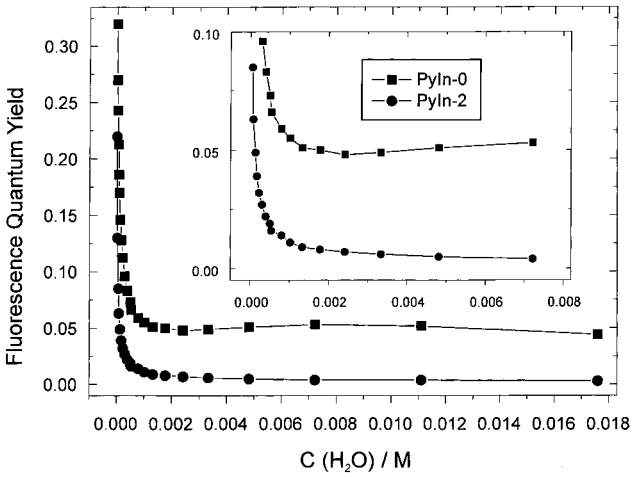


**Figure 12.** Changes in fluorescence quantum yields accompanying titration of acetonitrile solutions of **PyIn-0**, and **PyIn-2** with water at 293 K. Inset: middle portion of the plot, enhanced to show the appearance of a minimum for **PyIn-0**.

the appearance of water monomers, able to form 1:1 cyclic complexes with **7AI**. In our case, the presence of water monomers in mixed solvents could be a decisive factor for forming two independent hydrogen bonds with **PyIn-0**, thus promoting the *syn* → *anti* conformational change.

## Summary and Conclusions

Comparison of the photophysical properties of bridged and unbridged pyridylindoles in alcohol solvents allowed the detection of *syn* and *anti* rotamers, due to their different excited-state deactivation patterns. In **PyIn-0**, the *syn* → *anti* isomerization is promoted by the formation of two hydrogen bonds to two separate alcohol molecules. This leads to the stabilization of the *anti* form, in which two main deactivation paths (double proton transfer and $S_1 \rightarrow S_0$ internal conversion) dominant in the *syn* structure, are no longer possible. In another unbridged analogue, **DMPmIn-0**, the *syn* arrangement of the proton donor NH group and the pyrimidine nitrogen acceptor cannot be avoided. As a result, rapid deactivation is observed, similar to the case of methylene-bridged pyridylindoles.

A general scheme of processes occurring in both the ground and lowest excited singlet state of **PyIn-0** in alcohols is presented in Figure 13. A quite complicated pattern of emission results from the presence of at least two different types of alcohol complexes. The fluorescence of the *anti* forms ($F_1'$) is spectrally and kinetically different from the $F_1$ emission, due to the *syn* complexes. The latter fluorescence is efficiently quenched by $S_1 \rightarrow S_0$ internal conversion, occurring along the path from the noncyclic towards the cyclic solvates. Additional complexity is provided by the possibility that the $F_1$ band may not be homogeneous. If the *syn* population contains a fraction of cyclic complexes, they may rapidly decay by way of tautomerization. Overall, triply exponential decays are possible in alcohols, and these processes will be studied more closely, using pico- and femtosecond time-resolution.[37c]

In contrast to bulk alcohols, bulk water does not reveal the ability to form two independent hydrogen bonds to the donor and acceptor centers in **PyIn-0**. However, diluted water solutions in acetonitrile show hydrogen-bonding properties similar to those of alcohols.

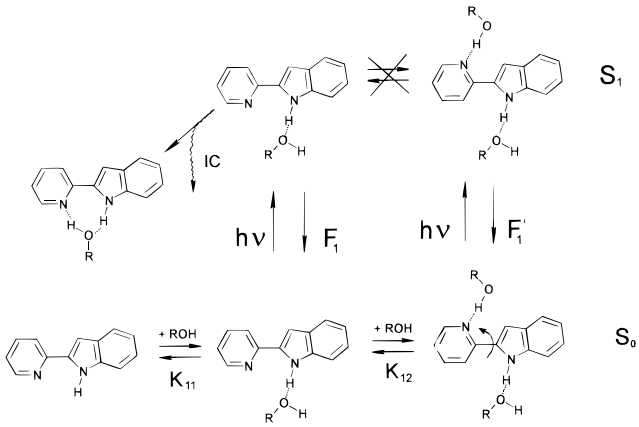


**Figure 13.** Scheme of ground and excited-state processes occurring in **PyIn-0** in the presence of hydroxylic solvents. $K_{11}$ and $K_{12}$ are the equilibrium constants of the formation of 1:1 and 1:2 alcohol complexes, respectively (see text); $F_1$ and $F_1'$ denote fluorescence from *syn* and *anti* conformers; IC indicates internal conversion.

A similar analysis of **3′-PyIn-0**, an isomer of **PyIn-0**, reveals the possible existence of a cyclic, triply hydrogen-bonded 1:2 alcohol complex in which proton transfer could occur according to a three-proton relay mechanism. Finally, the symmetry of a third isomer, **4′-PyIn-0**, dictates that it cannot form cyclic structures in alcohols, and as a consequence, its photophysics is totally solvent-insensitive.

A general observation of this work, confirming earlier results obtained for bridged derivatives,[34] is the inability of pyridylindoles to form cyclic 1:1 complexes in the ground state in bulk alcohols. Such structures are more readily formed, however, upon electronic excitation. In this respect pyridylindoles are very similar to 7-azaindole[21−24] and 1-azacarbazole (**1AC**),[69−72] but quite different from other close analogues, such as dipyrido-[2,3-*a*:3′,2′-*i*]carbazole (**DPC**), for which the presence of such cyclic solvates in the ground state has been demonstrated.[36] It remains to be seen whether theory can predict the ability to form cyclic complexes. Recent molecular dynamics calculations, comparing **7AI**, **1AC,** and **DPC**,[25] as well as our recent simulations comparing **PQ** with **PyIn-2**[37a] seem quite promising in this respect.

**Acknowledgment.** This work has been supported by the U.S.−Polish Maria Skłodowska-Curie Joint Fund II (Grant No. 97-305), the Robert A. Welch Foundation (E-621), the National Science Foundation (CHE-9714998), and by a grant from the Foundation for Polish Science ("Fastkin" program). Dr. Jacek Wójcik from the NMR facility of the Institute of Biochemistry and Biophysics of the Polish Academy of Sciences is gratefully acknowledged for performing the NOE measurements. Technical assistance of G. Orzanowska and A. Zielińska is greatly appreciated.

JA991818R

(68) Förster, T. *Z. Elektrochem. Ber. Bunsen-Ges. Phys. Chem.* **1950**, *54*, 42; Grabowski, Z. R.; Grabowska, A. *Z. Phys. Chem. NF* **1976**, *101*, 197.

(69) Chang, C.; Shabestary, N.; El-Bayoumi, M. A. Chem. Phys. Lett. **1980**, 75, 107.

(70) Waluk, J.; Grabowska, A.; Pakuła, B.; J.; Sepioł, J. *J. Phys. Chem.* **1984**, *88*, 1160.

(71) Waluk, J.; Komorowski, S. J.; Herbich, J. *J. Phys. Chem.* **1986**, *90*, 3868.

(72) Fuke, K.; Kaya, K. *J. Phys. Chem.* **1989**, *93*, 614.